Why (1*S*)-Camphanates Are Excellent Resolving Agents for Helicen-1-ols and Why They Can Be Used to Analyze Absolute Configurations

Tienthong Thongpanchang,[†] Kamil Paruch,[†] Thomas J. Katz,*[,†] Arnold L. Rheingold,[‡]
Kin-Chung Lam,[‡] and Louise Liable-Sands[‡]

Department of Chemistry, Columbia University, New York, New York 10027, and Department of Chemistry and Biochemistry, University of Delaware, Newark, Delaware 19716

Received December 20, 1999

The questions considered in this paper are why, as agents for resolving helicenols, camphanate esters are particularly effective, and why, in all 19 examples studied, when the (1*S*)-camphanates of (*P*)- and (*M*)-helicen-1-ols are chromatographed on silica gel, the former has the lower R_f. Models are proposed for the favored conformations of the esters, and to support the models, evidence is provided from five X-ray diffraction analyses and four ROESY analyses supplemented by molecular mechanics calculations. The essential discovery is that, presumably to avoid a steric interaction between a methyl on the camphanate's bridge and the helicene skeleton, the O=CCO conformation is anti-periplanar in (*M*)-helicenol camphanates and syn-periplanar in (*P*)-helicenol camphanates. In the former, the lactone carbonyl points toward the helicene ring system, and in the latter, it points away.

Introduction

To obtain helicenes in nonracemic form, the procedures used have been either to separate the enantiomers from racemic mixtures by techniques such as HPLC using chiral columns,[1] enzyme-catalyzed reactions,[2] complexation with chiral agents,[3] and selective crystallization of one enantiomer from a racemic mixture[4] or to synthesize one enantiomer selectively.[5] However, these procedures are either inappropriate for the preparation of large amounts or not generally applicable. The availability of helicenes in abundance and variety[2,6] has made it important to find ways to resolve their enantiomers in quantity, especially as nonracemic helicenes have a number of significant properties. These include material properties, such as the ability to self-assemble into chiral aggregates that exhibit large nonlinear optical responses and, when appropriately assembled, generate quasi-phase matched second harmonics[7] and properties useful for synthesis, such as the ability to act as chiral catalysts.[8]

Scheme 1

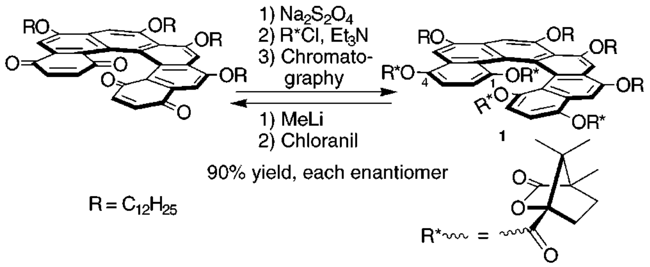

After studying a number of chiral derivatizing agents, Nuckolls found that to resolve a helicenebisquinone, tetracamphanates, prepared as summarized in Scheme 1, were more easily separated by chromatography than other esters. As also indicated in the scheme, the resolved camphanates were easily reconverted into the structure from which they were prepared.[6c,9] Camphanates have turned out to be outstandingly effective and generally applicable for the resolutions of helicenes. Examples are tetracamphanates derived from related [7]-carbo- and [7]-hetero-helicenebisquinones[6b,d] and di- and monocamphanates of helicen-1-ols, such as **2**,[10] **3**,[10] and **4**.[8] In each of these cases the (1*S*)-camphanate of the (*P*)-helicenol

---

[†] Columbia University.

[‡] University of Delaware.

(1) (a) Mikes, F.; Boshart, G.; Gil-Av, E. *J. Chem. Soc., Chem. Commun.* **1976**, 99. (b) Nakagawa, H.; Ogashiwa, S.; Tanaka, H.; Yamada, K.; Kawazura, H. *Bull. Chem. Soc. Jpn.* **1981**, *54*, 1903.

(2) Liu, L.; Katz, T. J. *Tetrahedron Lett.* **1990**, *31*, 3983.

(3) (a) Newman, M. S.; Lutz, W. B.; Lednicer, D. *J. Am. Chem. Soc.* **1955**, *77*, 3420. (b) Newman, M. S.; Lednicer, D. *J. Am. Chem. Soc.* **1956**, *78*, 4765. (c) Lightner, D. A.; Hefelfinger, D. T.; Powers, T. W.; Frank, G. W.; Trueblood, K. N. *J. Am. Chem. Soc.* **1972**, *94*, 3492.

(4) (a) Wynberg, H.; Groen, M. B. *J. Am. Chem. Soc.* **1968**, *90*, 5339. (b) Martin, R. H.; Marchant, M. J. *Tetrahedron* **1974**, *30*, 343.

(5) (a) Sudhakar, A.; Katz, T. J. *J. Am. Chem. Soc.* **1986**, *108*, 179. (b) Sudhakar, A.; Katz, T. J.; Yang, B.-W. *J. Am. Chem. Soc.* **1986**, *108*, 2790. (c) Katz, T. J.; Sudhakar, A.; Teasley, M. F.; Gilbert, A. M.; Geiger, W. E.; Robben, M. P.; Wuensch, M.; Ward, M. D. *J. Am. Chem. Soc.* **1993**, *115*, 3182. (d) Gilbert, A. M.; Katz, T. J.; Geiger, W. E.; Robben, M. P.; Rheingold, A. L. *J. Am. Chem. Soc.* **1993**, *115*, 3199. (e) Tanaka, K.; Osuga, H.; Suzuki, H. *Tetrahedron: Asymmetry* **1993**, *4*, 1843. (f) Osuga, H.; Suzuki, H.; Tanaka, K. *Bull. Chem. Soc. Jpn.* **1997**, *70*, 891.

(6) (a) Katz, T. J.; Liu, L.; Willmore, N. D.; Fox, J. M.; Rheingold, A. L.; Shi, S.; Nuckolls, C.; Rickman, B. H. *J. Am. Chem. Soc.* **1997**, *119*, 10054. (b) Fox, J. M.; Goldberg, N. M.; Katz, T. J. *J. Org. Chem.* **1998**, *63*, 7456. (c) Nuckolls, C.; Katz, T. J.; Katz, G.; Collings, P. J. Castellanos, L. *J. Am. Chem. Soc.* **1999**, *121*, 79. (d) Dreher, S. D.; Weix, D. J.; Katz, T. J. *J. Org. Chem.* **1999**, *64*, 3671.

(7) (a) Nuckolls, C.; Katz, T. J. *J. Am. Chem. Soc.* **1998**, *120*, 9541. (b) Nuckolls, C.; Katz, T. J.; Verbiest, T.; Van Elshocht, S.; Kuball, H.-G.; Kiesewalter, S.; Lovinger, A. J.; Persoons, A. *J. Am. Chem. Soc.* **1998**, *120*, 8656. (c) Verbiest, T.; Van Elshocht, S.; Kauranen, M.; Hellemans, L.; Snauwaert, J.; Nuckolls, C.; Katz, T. J.; Persoons, A. *Science (Washington, D.C.)* **1998**, *282*, 913. (d) Fox, J. M.; Katz, T. J.; Van Elshocht, S.; Verbiest, T.; Kauranen, M.; Persoons, A.; Thongpanchang, T.; Krauss, T.; Brus, L. *J. Am. Chem. Soc.*, **1999**, *121*, 3453. (e) Busson, B.; Kauranen, M.; Nuckolls, C.; Katz, T. J.; Persoons, A. *Phys. Rev. Lett.* **2000**, *84*, 79.

(8) Dreher, S. D.; Katz, T. J.; Lam, K.-C.; Rheingold, A. L. *J. Org. Chem.* **2000**, *65*, 806.

(9) Nuckolls, C.; Katz, T. J.; Castellanos, L. *J. Am. Chem. Soc.* **1996**, *118*, 3767.

10.1021/jo9919411 CCC: $19.00

moves more slowly upon chromatography on silica gel than the (1*S*)-camphanate of the (*M*)-helicenol. Moreover, in two examples studied so far, **2** and **4**, in which the side chains are very small—methoxyls rather than, as in Scheme 1, dodecyloxyls—the more polar camphanate crystallizes from solvents of low polarity, making the resolutions particularly easy.[11]

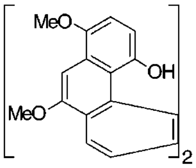

2

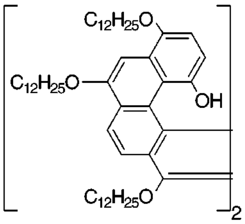

3

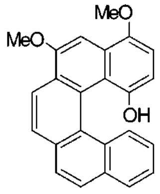

4

The questions considered in this paper are why camphanate esters of helicenols are so effective as resolving agents and why the (1*S*)-camphanates of (*P*)-helicen-1-ols always appear to be more polar than their (*M*)-diastereomers. Models are proposed for the favored conformations of the esters, and evidence from X-ray diffraction analyses and NMR analyses, supplemented by molecular mechanics calculations, is provided to support these models. The theoretical understanding provides a basis for the hypothesis that thin layer chromatograms can be used to assign absolute configurations to helicenes, and it may provide a basis for the future design and selection of resolving agents.

Results

It is the camphanates attached to the insides of the helicenes, for example, in **1** to the 1-position rather than to the 4-position, that appear to play the dominant role in effecting the resolutions. The evidence is the observation cited above that diastereomers that lack 4-camphanate groups, such as the camphanates of **2** and **4**, are easily separated. In addition, there is an example, a [7]-helicene structure, in which dicamphanates (**15** below) are much easier to separate than the tetracamphanates (the analogues with structures related to **1**).[12] It is also reasonable that the camphanates on the inside would be most sensitive to the structure of the helicene because the crowding there should restrict their motion. Accordingly, it is the conformations of camphanates attached to the 1-positions of helicenes that are analyzed below, and the helicenes chosen for the analysis are those with six rings.

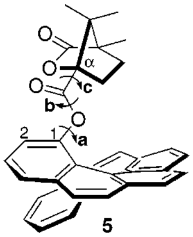

5

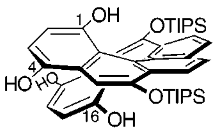

6

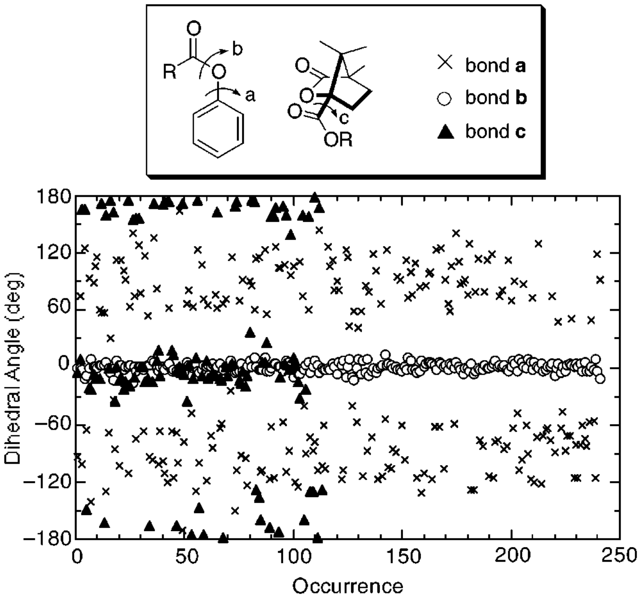

Figure 1. Preferred conformations of bonds **a** and **b** in phenyl esters and **c** in camphanate esters for structures in the Cambridge Structural Database.

A Model for the Lowest Energy Conformations of the Camphanates of Helicen-1-ols. Consider the camphanate of a helicen-1-ol, pictured in structure **5**, which has side chains removed for clarity. The orientation of the camphanate with respect to the ring system is determined by the dihedral angles about three single bonds, **a**, **b**, and **c**. The angles are defined, respectively, as C_2-C_1-O-C, $C_1-O-C=O$, and $O=C-C_\alpha-O$. Although only three aryl camphanates have been analyzed by diffraction,[13] the structures of many phenol esters have been, and their dihedral angles analogous to **a** and **b** are displayed graphically in Figure 1.[14] The figure also displays values of the dihedral angles analogous to **c**, as measured from the diffraction analyses of a variety of camphanate esters. The figure shows that the carbonyl groups of phenol esters do not lie in the planes of the benzene rings. Instead, the preferred angles **a** are 92 ± 26° and −90 ± 27°, in accord with previous NMR spectroscopic and theoretical analyses.[15,16] Steric repulsions between the carbonyl oxygens and the phenyl's C-2 hydrogens are thought to be the determinants.[15,16] Thus in **5**, the C=O bond must point either down, toward the aromatic rings at the other end of the helicene, or up, away from the helicene framework. Both space-filling models and calculations to be described below, using the MacroModel molecular mechanics program[17] with the MM3* force field,[18] imply that the preferred orientation should be the latter, in which the carbonyl points away

---

[10] Dreher, S. D.; Paruch, K.; Katz, T. J. *J. Org. Chem.* **2000**, *65*, 815.

[11] The (+)-(1*S*)-camphanate of **2** crystallizes from 1:1 cyclohexane/EtOAc.[10] The (+)-(1*S*)-camphanate of **4** is insoluble in ether.[8]

[12] Paruch, K.; Katz, T. J.; Incarvito, C.; Rheingold, A. L., unpublished results.

[13] One is a dicamphanate; the others are monocamphanates. (a) Li, H.-Y.; Nehira, T.; Hagiwara, M.; Harada, N. *J. Org. Chem.* **1997**, *62*, 7222. Results found were **a** = −72°, **b** = 11°, **c** = 10° and **a** = −62°, **b** = −6°, **c** = 176°. (b) Fuji, K.; Sakurai, M.; Kinoshita, T.; Kawabata, T. *Tetrahedron Lett.* **1998**, *39*, 6323. Results found were **a** = −57°, **b** = −15°, **c** = 7°. (c) Ohmori, K.; Kitamura, M.; Suzuki, K. *Angew. Chem., Int. Ed. Engl.* **1999**, *38*, 1226. Results found were **a** = −100.8°, **b** = 2.9°, **c** = 2.4°.

[14] Data from the Cambridge Structural Database (Allen, F. H.; Kennard, O. *Chemical Design Automation News* **1993**, *8*, 1 and 33).

[15] Schaefer, T.; Penner, G. H. *Can. J. Chem.* **1987**, *65*, 2175.

[16] Schaefer, T.; Sebastian, R.; Penner, G. H. *Can. J. Chem.* **1988**, *66*, 1787.

[17] Mohamadi, F.; Richards, N. G. J.; Guida, W. C.; Liskamp, R.; Lipton, M.; Caufield, C.; Chang, G.; Hendrickson, T.; Still, W. C. *J. Comput. Chem.* **1990**, *11*, 440.

from the helicene framework. So does a similar calculation that searched for the lowest energy conformation of structure **5** but with formate in place of camphanate.

Figure 1 shows that the dihedral angle that defines **b** is 0 ± 5°. That is, esters exhibit a strong preference for bonds such as $O-C_1$ to eclipse the carbonyl group, a preference that is well-known[19] and has been attributed to dipole–dipole interactions between the polar $C{=}O$ and $O-C$ bonds[20] and to hyperconjugation of an ether oxygen lone pair with a σ^* orbital of the carbonyl group.[19a,21] Accordingly, bond **b** in the helicene structures should have the s-trans conformation.

Since dihedral angles **a** and **b** should be the same in the right-handed and left-handed helicenes, only a difference in angle **c** can alter the orientation of the camphanate with respect to the ring systems. In other words, *it must be a change in angle* **c** *that is the origin of the change in polarity that is observed*. As Figure 1 shows, in crystalline camphanates, angle **c** is close either to 0° (the measured figures are 12 ± 8°) or to $180° \equiv -180°$ (the measured figures are 180 ± 22°). Moreover, it is plausible that the conformation about this bond should be similar to that of the bond between the carbonyl carbon and the α-carbon of methoxyacetates, and for this bond, both theory and spectroscopy imply that these two conformations are preferred[22,23] and that they are similar in energy.[22a] The carbon–ether bond and the carbonyl should be either syn-periplanar (**c** = 0°) or anti-periplanar (**c** = 180°). Tucker, Houk, and Trost attributed these preferences to the stabilization being greater when the electron-deficient $C{=}O$ π-bond is hyperconjugated with a $C-H$ rather than with a $C-O$ bond, even though the $C-O$ must then most strongly repel the $C{=}O$ both sterically and electrostatically.[22a] The conclusion is that in the helicene camphanate **5**, the preferred rotational phase about **c** should have the $C_\alpha-O$ bond either syn-periplanar or anti-periplanar to the carbonyl.

To analyze which of these two should be preferred in the helicene structures, models were constructed of the (1*S*)-camphanates of (*M*)- and (*P*)-helicen-1-ols. Angles **a** and **b** were set to 90° and 0°, respectively. Figure 2 shows that in the (*M*)-helicene there is a steric interaction between one of the bridge methyl groups and the ring system when **c** = 0° and that it is relieved when **c** = 180°. Accordingly, the latter should be the favored conformation, and it has the lactone group pointing down, toward the helicene ring system. In the (*P*)-helicene, the reverse should be true. Figure 3 shows that in this structure there is also a steric interaction between the same bridge methyl group and the ring system, but not, as in the (*M*)-helicene, when **c** is 0°. It occurs when **c** is 180°, and it is relieved when **c** is 0°. The consequence is that in the (*P*)-helicenes the favored conformation should have the lactone group pointing up, away from the helicene core. It is, therefore, reasonable that when the helicene (1*S*)-camphanates are chromatographed on silica gel, the (*P*)-isomer has the lower R_f.

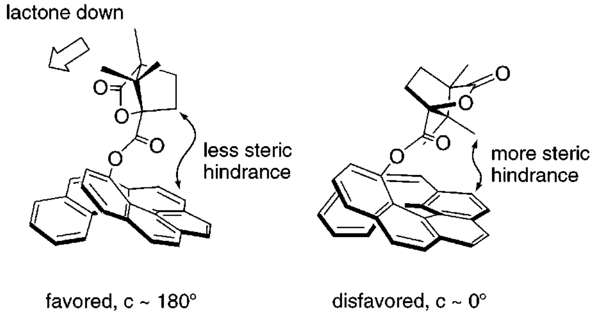

Figure 2. Models showing the orientation of the camphanate with respect to the (*M*)-helicene ring system to which it is attached at position 1, when **c** = 180° and when **c** = 0°. Angles **a** and **b** are 90° and 0°, respectively.

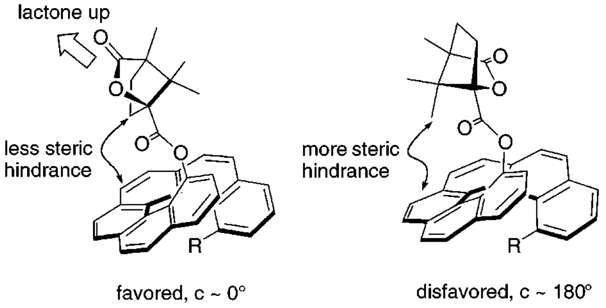

Figure 3. Models showing the orientation of the camphanate with respect to the (*P*)-helicene ring system to which it is attached at position 1, when **c** = 0° and when **c** = 180°. Angles **a** and **b** are 90° and 0°, respectively.

Evidence from ROESY. The tetra-(1*S*)-camphanate esters of **6** were separated by chromatography on silica gel into the faster-moving diastereomer, (*M*)-**7**, and the slower-moving diastereomer, (*P*)-**8**, the former levorotatory ($[\alpha]_D$ −600, *c* 0.0244, CH_3CN) and the latter dextrorotatory ($[\alpha]_D$ +430, *c* 0.0222, CH_3CN). Their absolute configurations could be assigned definitively because the structure of a derivative of **8** (structure **11** below) was analyzed by X-ray diffraction. Their ^1H NMR spectra are displayed in Figure 4, which also shows to which protons the resonances were assigned.

The resonance of H_5 is easily identified because it is the only singlet. The doublets at the high-field end of the aromatic region are assigned to H_2 and H_3 both because phenol esters shift ortho protons to high fields[24] and because H_2 and H_3 are the protons that in [6]helicenes resonate at highest fields.[25] Of these, H_2 is assigned to

---

(18) Allinger, N. L.; Yuh, Y. H.; Lii, J.-H. *J. Am. Chem. Soc.* **1989**, *111*, 8551.

(19) (a) Deslongchamps, P. *Stereoelectronic Effects in Organic Chemistry*; Pergamon Press: Oxford, 1983; Vol. 1. (b) Jones, G. I. L.; Owen, N. L. *J. Mol. Struct.* **1973**, *18*, 1. (c) Oki, M.; Nakanishi, H. *Bull. Chem. Soc. Jpn.* **1970**, *43*, 2558. (d) Wiberg, K. B.; Laidig, K. E. *J. Am. Chem. Soc.* **1987**, *109*, 5935. (e) Coulter, P.; Windle, A. H. *Macromolecules* **1989**, *22*, 1129.

(20) Wennerström, H.; Forsén, S.; Roos, B. *J. Phys. Chem.* **1972**, *76*, 2430.

(21) Larson, J. R.; Epiotis, N. D.; Bernardi, F. *J. Am. Chem. Soc.* **1978**, *100*, 5713.

(22) (a) Tucker, J. A.; Houk, K. N.; Trost, B. M. *J. Am. Chem. Soc.* **1990**, *112*, 5465, and reference therein. (b) Dale, J. A.; Mosher, H. S. *J. Am. Chem. Soc.* **1973**, *95*, 512. (c) Trost, B. M.; Belletire, J. L.; Godleski, S.; McDougal, P. G.; Balkovec, J. M.; Baldwin, J. J.; Christy, M. E.; Ponticello, G. S.; Varga, S. L.; Springer, J. P. *J. Org. Chem.* **1986**, *51*, 2370. (d) Siegel, C.; Thornton, E. R. *Tetrahedron Lett.* **1988**, *29*, 5225. (e) Siegel, C.; Thornton, E. R. *Tetrahedron: Asymmetry* **1991**, *2*, 1413.

(23) (a) Latypov, S. K.; Seco, J. M.; Quiñoá, E.; Riguera, R. *J. Org. Chem.* **1995**, *60*, 504. (b) Latypov, S. K.; Ferreiro, M. J.; Quiñoá, E.; Riguera, R. *J. Am. Chem. Soc.* **1998**, *120*, 4741 and references therein.

(24) (a) Bovey, F. A.; Jelinski, L.; Mirau, P. A. *Nuclear Magnetic Resonance Spectroscopy*, 2nd ed.; Academic Press: San Diego, 1988; p 138. (b) Robinson, J. W., Ed.; *CRC Handbook of Spectroscopy, Vol. II*; CRC Press: Cleveland, Ohio, 1974; p 331.

(25) (a) Laarhoven, W. H.; Prinsen, W. J. C. *Top. Curr. Chem.* **1984**, *125*, 63. (b) Defay, N.; Martin, R. H. *Bull. Soc. Chim. Belg.* **1984**, *93*, 313 and references therein.

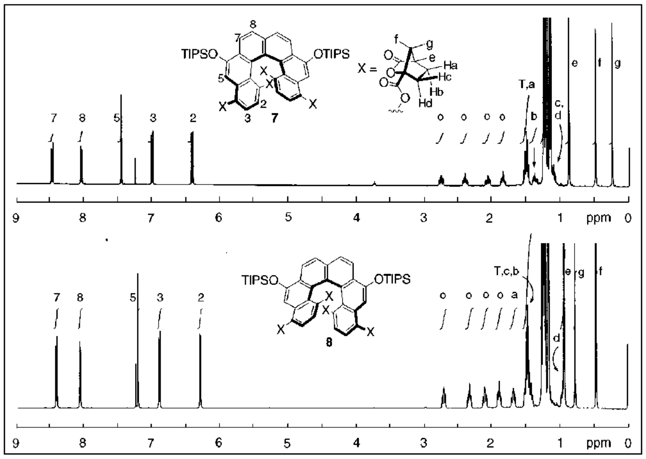

Figure 4. ^{1}H NMR (500 MHz) spectra of the tetra(1*S*)-camphanates of **6** in CDCl$_3$. Top: **7**, the (−)-diastereomer; bottom: **8**, the (+)-diastereomer. Peak assignments are shown. The symbol “o” identifies methylene resonances of the camphanates attached to position 4 (the outside); “T” identifies isopropyl resonances of the TIPS groups.

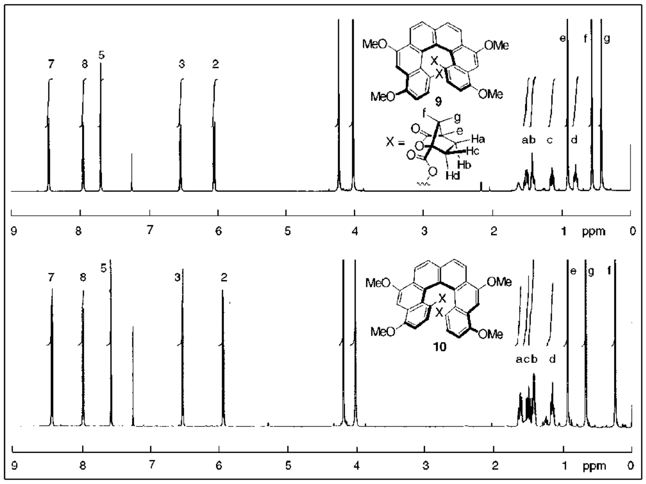

Figure 5. ^{1}H NMR (500 MHz) spectra of the tetra(1*S*)-camphanates of **2** in CDCl$_3$. Top: **9**, the (−)-diastereomer, which moves faster when chromatographed on silica gel; bottom: **10**, the (+)-diastereomer, which moves slower. Peak assignments are shown.

the peak at the highest field by analogy with the spectra of other [6]helicenes.[25] Also in accord with the ^{1}H NMR chemical shifts of [6]helicene,[25] the doublets at lowest field are assigned to H$_7$ and H$_8$, and of these, the resonance at the lowest field is assigned to H$_7$ because it is at lower fields than the corresponding resonance of [6]-helicene, an effect that can be attributed to the peri-TIPSO group.[26] Of the resonances attributable to the camphanate groups, the three singlets at highest fields are assigned to the methyls of the camphanates that are attached to the inside of the helix, at positions 1 and 16 (see structure **6** for the numbering). The reason is that such resonances also appear in the spectra of the dicamphanates of **2** [(*M*)−(−)-**9** and (*P*)−(+)-**10**, Figure 5],[10] which have camphanate groups only on the insides of the helix skeletons. The resonances in Figure 4 between δ 1.9 and 2.8 must be assigned to the methylenes of camphanates on the outsides of the helicenes, for these resonances are absent in Figure 5.

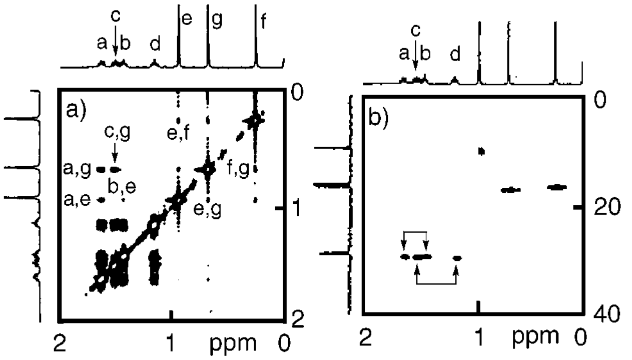

Figure 6. (a) ROESY (500 MHz) and (b) HMQC spectra of the camphanate fragment of **10**.

The absolute configurations could be assigned unambiguously to **9** and **10** because the structure of **10**, as shown below, was analyzed by X-ray diffraction. The only significant differences in the ^{1}H NMR spectra of diastereomers **7** and **8** (Figure 4) and **9** and **10** (Figure 5) are, among the aromatic resonances, a shift of the singlet due to the resonance of H$_5$ to lower fields (by 0.25 ppm) in the (*P*)−(+)-diastereomers and, among the camphanate resonances, a shift of the resonances at highest fields due to the methyls of the inside camphanates. The resonances of the outside camphanates, displayed in Figure 4, are similar in the two diastereomers and similar to those of *p*-methoxyphenyl camphanate, whose spectrum is displayed in the Supporting Information.

Evidence that the camphanates in **7**−**10** adopt the orientation that should be favored according to Figures 2 and 3 is provided by rotating-frame Overhauser enhancement spectroscopy experiments (ROESY).[27] For this analysis to be carried out, the chemical shifts had to be assigned to the protons of the groups attached to carbons 1 and 16. Interactions between the methyl and methylene protons of these camphanates provided a basis for the assignments. Figure 6a displays the ROESY spectrum of the camphanate protons of **10**. Overhauser enhancements are observed between H$_e$ and H$_a$, H$_e$ and H$_b$, H$_g$ and H$_a$, and H$_g$ and H$_c$. None is observed between H$_f$ and any other methylene proton, which is reasonable since H$_f$, uniquely among the methyl groups, points away from the methylenes.

The ROESY analysis in Figure 6a suffices to identify the resonances of both H$_a$ and H$_d$. H$_a$ shows cross-peaks with two methyl protons, while H$_d$ shows cross-peaks with none. Because both H$_b$ and H$_c$ show cross-peaks with a single methyl, further analysis is required to distinguish them. The ^{1}H-detected heteronuclear multiple-quantum coherence (HMQC) spectrum[27a] in Figure 6b shows that H$_b$ is attached to the same carbon as H$_a$. Similarly, H$_c$ is attached to the same carbon as H$_d$. The assignments of methyls e and g then follow from their ROESY cross-peaks.

---

(26) (a) Wang, Z.; Yang, S.; Yang, Y.; Bi, Y. *Fenxi Huaxue* **1984**, *12*, 489; *Chem. Abstr.* **1985**, 131443. (b) Robinson, J. W., Ed.; *CRC Handbook of Spectroscopy, Vol. II*; CRC Press: Cleveland, Ohio, 1974; p 338. (c) Lucchini, V.; Wells, P. R. *Org. Magn. Reson.* **1976**, *8*, 137.

(27) (a) Croasmun, W. R.; Carlson, R. M. K. *Two-dimensional NMR Spectroscopy: Applications for Chemists and Biochemists*, 2nd ed.; VCH: New York, 1994. (b) Bothner-By, A. A.; Stephens, R. L.; Lee, J.-M. *J. Am. Chem. Soc.* **1984**, *106*, 811. (c) Günther, H. *NMR Spectroscopy*, 2nd ed.; Wiley: New York, 1995. (d) Nakanishi, K. *One-dimensional and Two-dimensional NMR Spectra by Modern Pulse Techniques*; University Science Books: Tokyo, 1990.

Table 1. Structural Parameters for Eight 1-Helicenol (1*S*)-Camphanates According to Simple Analogies, Distance Constrained Molecular Mechanics Calculations, and X-Ray Diffraction Analyses[a]

angles (deg) and distances (Å)	(*M*)-isomers					(*P*)-isomers					
	analogy	calcd **7**	calcd **9**	X-ray **11**	X-ray **14**	analogy	calcd **8**	calcd **10**	X-ray **10**	X-ray **13**	X-ray **15**
a	~90	85	99	82	95	~90	−86	−69	−90	−90	−102
b	0	4	6	5	12	0	−10	−3	−12	−6	−12
c	~180	−174	−178	−155	−131	~0	−43	−31	−14	−8	−18
H_2−H_f	<5	2.9	3.1	2.9	4.1	<5	3.9	3.3	2.9	3.0	3.4

[a] The figures are average values for the two inside camphanate groups.

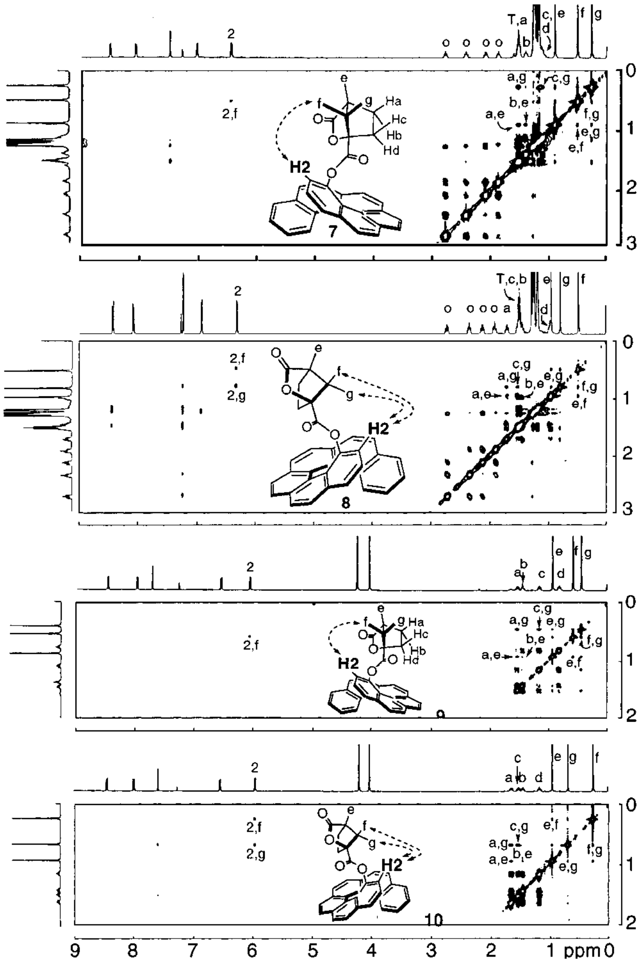

Figure 7. ROESY (500 MHz) spectra and chemical shifts assignment for **7**−**10**. Only the camphanates attached to C-1 are shown. Side chains and outside camphanates have been deleted for clarity. The methylene proton resonances of the outside camphanates are identified by “o”; the isopropyl resonances of the TIPS groups are identified by “T”.

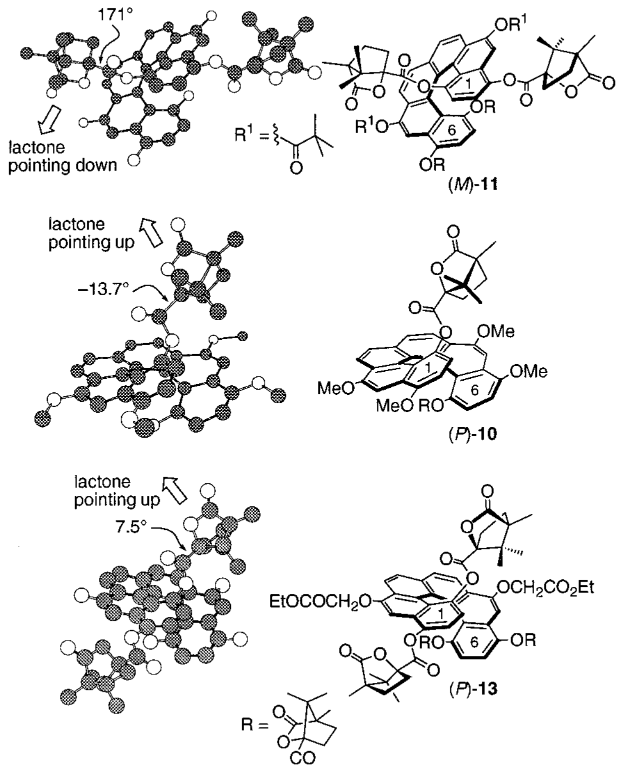

Figure 8. Structures of **10**, **11**, and **13**: on the left according to X-ray diffraction analyses and on the right according to conventional drawings. Side chains and camphanate groups attached to ring 6 are omitted for clarity. Oxygen atoms are represented in white.

Figure 7 shows the ROESY analyses of **7**−**10**, with the resonances assigned as discussed above to the protons of the inside camphanates and to H_2. Each spectrum shows a cross-peak between H_2 of the helicene skeleton and the protons of methyl f on the inside camphanate group. This means that these two protons can be no further apart than 5 Å.[27a] Accordingly, the MacroModel program described above was used to search for the lowest energy conformations that had this constraint imposed. The structures are in the Supporting Information, and their relevant bond angles are summarized in Table 1.

X-ray Diffraction Analyses. The orientations of the camphanates were analyzed by X-ray diffraction. Suitable crystals could be grown of **10** but not of **7**, **8**, or **9**. Therefore, the side chains of **7** and **8** were modified in the hope that crystal growth would be enhanced. By combining **7** and **8** in THF with tetrabutylammonium fluoride and pivaloyl chloride, **11** and **12** were obtained in yields of 72% and 75%. However, of these two, only **11** formed crystals (from methanol-hexanes) suitable for X-ray diffraction analysis. Although **12** did not, a different derivative of **8** that was prepared in the course of other work,[28] **13**, did form good crystals (from hexanes−ethyl acetate). Accordingly, the structures of **10**, **11**, and **13** were analyzed by X-ray diffraction. These structures, and in particular the conformations of the camphanates, are displayed in Figure 8.

Discussion

Table 1 summarizes significant angles and distances in (*M*)-**11**, (*P*)-**10**, and (*P*)-**13** according to three analyses: the most simple analogy, the distance-constrained conformational analysis, and the X-ray diffraction analysis. The distance-constrained conformational analyses supplement those for the related **7**−**9**, which were considered earlier. In addition, the table includes relevant

---

(28) Thongpanchang, T., unpublished results.

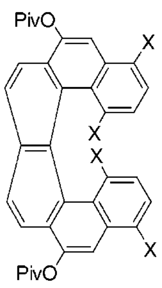

11 : (*M*)-(−)
12 : (*P*)-(+)

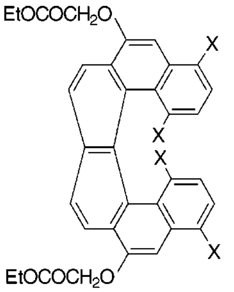

13 : (*P*)-(+)

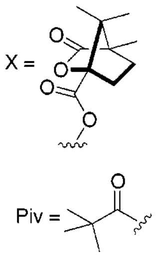

data from X-ray diffraction analyses of two other (1*S*)-camphanates, an (*M*)-[5]helicen-1-ol (**14**),[8] and a (*P*)-[7]-helicenediol (**15**),[12] which were prepared and analyzed in the course of other work. Regarding the data in Table 1, essential observations are that the figures provided by the molecular mechanics calculations and by the X-ray diffraction analyses are similar to each other and similar to those expected according to the most simple analogy. Most important, the angle **c**, between the bicyclo[2.2.1]-ring system and its attached carbonyl, is small when the helicene has the (*P*)-configuration and large when it has the (*M*)-configuration.

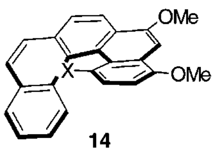

14

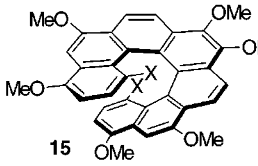

15

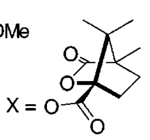

This means that the lactone group points away from a (*P*)-helicene and toward an (*M*)-helicene. That would account for why the resonances of the protons on carbons 5 in **7**−**10** (as displayed in Figures 4 and 5), as well as of the analogous protons in other helicenes (as summarized in Table S1 in the Supporting Information), are at higher fields in the *P*-isomers than in the *M-isomers*. Notice that carbon 5 is the same as carbon 12 when counting is started from the other end of the molecule. The calculational procedure of Abraham shows that when the lactone points toward the helicene, the proton on carbon 12 is in a deshielding region of the carbonyl group.[29] More important is that the inside lactones of the (*P*)-helicenol (1*S*)-camphanates are exposed to the silica surface. A quantitative measure is the area of a camphanate's lactone that is accessible to water solvent, and this is calculated[30] to be much larger in the (*P*)-helicene **8** (54 Å^2) than in its (*M*)-diastereomer, **7** (28 Å^2). Accordingly, it is reasonable that upon chromatography on silica gel, it is the former helicene that moves more slowly. Indeed, as summarized in the Supporting Information, 19 helicen-1-ol (1*S*)-camphanates with 5−7 rings, some with skeletons that are only carbon and some with skeletons that include heteroatoms, have been separated and analyzed, and in every case, the diastereomer in which the helix winds to the right moves more slowly upon chromatography on silica gel. Accordingly, their thin layer chromatograms alone suffice to assign the absolute stereochemistries to such compounds. Compared to other methods for determining absolute configurations,[31] this must be the easiest and require the least amount of material. Furthermore, the analysis described above might extend to molecules other than helicenes, and it could provide a basis for rationally designing resolving agents.

Conclusions

Analyses both by ROESY supplemented by molecular mechanics calculations and by X-ray diffraction verify the hypothesis derived from analogies and molecular models, that the O=CCO conformation is anti-periplanar in (*M*)-helicen-1-ol camphanates and syn-periplanar in (*P*)-helicen-1-ol camphanates. In the former, the lactone carbonyl points toward the helicene ring system, and in the latter away. This accounts for why the R_f is lower when the helicene has the *P*-configuration.

Experimental Section

THF and toluene were distilled from Na/benzophenone, CH_2Cl_2 and Et_3N from CaH_2. Zinc dust (Aldrich, <10 μm, 98+%) was activated prior to use.[32] (1*S*)-(−)-Camphanoyl chloride (98%), tetrabutylammonium fluoride (1 M solution in THF), and trimethylacetyl chloride (99%) were purchased from Aldrich and used without purification. Glassware was flame-dried under vacuum and cooled under N_2. Reactions were run under N_2. Additions by syringe were through rubber septa. "Chromatography" refers to flash chromatography.[33] The matrix for FAB mass spectrometry was *m*-nitrobenzyl alcohol.

The instrument used to record the 2D ROESY and HMQC NMR spectra was a Bruker 500 Fourier transform spectrometer. The mixing time for the ROESY experiments was 200 ms. Silica gel F-254 precoated plates from Scientific Adsorbents, Inc. were used for thin-layer chromatography (TLC).

The MacroModel V.6.0 program with MM3* force field, operating on a Silicon Graphics-Indy computer, was used for the Monte Carlo molecular mechanics conformation searches. Initially, a structure of local minimum energy was calculated for **7**−**10**. The frameworks of both the helicene and the camphanate moieties were then rigidly preserved. The remaining torsion angles were varied in 1000 Monte Carlo steps with the distance between H_2 and the protons of methyl f constrained to be less than 5 Å. At each of these steps, the energy was minimized. Once the structure of global minimum energy was found, the MacroModel program was used to analyze its angles and distances.

Crystallographic Studies. The crystal data collection and refinement parameters are in Table 2. The systematic absences in the diffraction data of **10** and **11** were uniquely consistent for orthorhombic space group, $P2_12_12_1$. For **13**, the diffraction data provided no evidence of symmetry higher than triclinic. Account of *E*-statistics and of **13** being nonracemic suggested the space group option *P*1, which yielded chemically reasonable and computationally stable results on refinement. The structures were solved using direct methods, completed by subsequent difference Fourier syntheses, and refined by full-matrix, least-squares procedures. Empirical *SADABS* absorption corrections were applied to all data sets. The asymmetric units of **10**, **11**, and **13** contain, respectively, two molecules of ethyl acetate, one of methanol, and one of ethyl acetate. All non-hydrogen atoms were refined with anisotropic displacement coefficients, and all hydrogen atoms were treated as idealized contributions. The absolute configurations could be assigned because those of the camphanate moieties were known.

The software and the sources of the scattering factors are contained in the SHELXTL (5.10) program library (G. Sheldrick, Siemens XRD, Madison, WI).

---

(29) Abraham, R. J. *Prog. Nucl. Magn. Reson. Spectrosc.* **1999**, *35*, 85.

(30) (a) Lee, B.; Richards, F. M. *J. Mol. Biol.* **1971**, *55*, 379. (b) Hermann, R. B. *J. Phys. Chem.* **1972**, *76*, 2754. The probe size was 1.4 nm.

(31) Eliel, E. L.; Wilen, S. H.; Mander, L. W. *Stereochemistry of Organic Compounds*; Wiley: New York, 1994; Chapters 5 and 13.

(32) Shriner, R. L.; Neumann, F. W. *Organic Syntheses*; Wiley: New York, 1955; Collect. Vol. III, p 73.

(33) Still, W. C.; Kahn, M.; Mitra, A. *J. Org. Chem.* **1978**, *43*, 2923.

Table 2. Crystallographic Data for $C_{50}H_{48}O_{12}$ (10)·EtOAc, for $C_{76}H_{80}O_{20}$ (11)·MeOH, and for $C_{74}H_{76}O_{22}$ (13)·2EtOAc

	10·EtOAc	**11**·MeOH	**13**·2EtOAc
formula	$C_{54}H_{56}O_{14}$	$C_{77}H_{84}O_{21}$	$C_{82}H_{92}O_{26}$
formula weight	904.97	1345.44	1493.56
space group	$P2_12_12_1$	$P2_12_12_1$	$P1$
a, Å	11.3435(2)	11.2580(2)	11.1849(2)
b, Å	16.5631(2)	21.3657(3)	11.3784(2)
c, Å	25.9780(2)	28.6534(4)	16.4757(3)
α, deg			106.4516(2)
β, deg			102.5875(8)
γ, deg			103.0782(7)
V, Å^3	4880.84(6)	6892.1(3)	1867.41(2)
Z, Z′	4	4	1
cryst color, habit	yellow prism	yellow plate	yellow block
D(calc), g/cm^3	1.232	1.297	1.328
μ(Mo Kα), cm^{-1}	0.91	0.94	0.99
temp, K	173(2)	173(2)	173(2)
diffractometer	Siemens P4/CCD		
radiation	MoKα ($\lambda = 0.71073$ Å)		
R (F), %^{a}	6.53	6.91	5.33
R (wF^2)·%^{a}	14.73	18.82	18.26

[a] Quantity minimized = $R(wF^2) = \Sigma[w(F_o^2 - F_c^2)^2]/\Sigma[(wF_o^2)^2]^{1/2}$; $R = \Sigma\Delta/\Sigma(F_o)$, $\Delta = |(F_o - F_c)|$; $w = 1/[\sigma^2(F_o^2) + (aP)^2 + bP]$, $P = [2F_c^2 + \mathrm{Max}(F_o, 0)]/3$.

Preparation of (*M*)-(−)-7 and (*P*)-(+)-8. Et_3N (2 mL) and activated[32] Zn (1.12 g, 17.1 mmol) were added to a solution of the bisquinone of **6**[10] (500 mg, 0.683 mmol) and (1*S*)-(−)-camphanoyl chloride (1.48 g, 6.83 mmol) in 30 mL of CH_2Cl_2. The mixture was stirred at 25 °C overnight. Filtration through Celite, aided by several ethyl acetate washes, removed remaining Zn. The yellow organic solution was washed with saturated aqueous $NaHCO_3$ (2×), 1 N HCl, and H_2O and dried (Na_2SO_4). Removal of solvent left a slightly brown yellow wax, from which chromatography using 1:2 ethyl acetate/hexanes as an eluent yielded 755 mg (76% yield) of the high R_f isomer (*M*)-**7** (a yellow solid, mp > 250 °C) and 806 mg (81% yield) of the low R_f isomer (*P*)-**8** (a yellow solid, mp > 250 °C).

(*M*)-7: $[\alpha]_D$ −600 (c 0.0244, CH_3CN); IR (CCl_4) 2967, 1797, 1753, 1262, 1048 cm^{-1}; ^{1}H NMR ($CDCl_3$, 400 MHz) δ 8.47 (d, J = 8.4 Hz, 2H), 8.05 (d, J = 8.4 Hz, 2H), 7.49 (s, 2H), 7.01 (d, J = 8.4 Hz, 2H), 6.42 (d, J = 8.4 Hz, 2H), 2.77 (m, 2H), 2.41 (m, 2H), 1.86 (m, 2H), 1.51 (m, 8H), 1.39 (m, 2H), 1.3−1.1 (m, 58H), 0.89 (s, 6H), 0.50 (s, 6H), 0.25 ppm (s, 6H); ^{13}C NMR ($CDCl_3$, 75 MHz) 178.1, 177.4, 166.1, 164.4, 151.1, 144.0, 142.7, 131.2, 128.4, 127.4, 126.9, 126.0, 124.4, 121.4, 120.7, 118.4, 115.0, 105.6, 91.1, 89.6, 55.0, 54.5, 54.3, 54.0, 31.0, 29.1, 29.0, 28.7, 18.2, 17.0, 16.9, 16.1, 15.8, 13.0, 9.8, 9.6 ppm; UV−vis (CH_3CN, $c = 2.8 \times 10^{-5}$ M) λ_{max} (log ϵ) 266 (6.38), 326 (6.21), 407 (5.30), 431 (5.37); CD (CH_3CN, $c = 2.8 \times 10^{-5}$ M), nm ($\Delta\epsilon$) 228 (−39), 259 (108), 300 (−35), 316 (8), 346 (−101), 433 (6); HRMS (FAB) m/z calcd for $C_{84}H_{104}O_{18}Si_2$ 1456.6761, found 1456.6796.

(*P*)-8: $[\alpha]_D$ +430 (c 0.0222, CH_3CN); IR (CCl_4) 2965, 1801, 1757, 1260, 1044 cm^{-1}; ^{1}H NMR ($CDCl_3$, 400 MHz) δ 8.43 (d, J = 8.5 Hz, 2H), 8.08 (d, J = 8.5 Hz, 2H), 7.22 (s, 2H), 6.91 (d, J = 8.3 Hz, 2H), 6.31 (d, J = 8.3 Hz, 2H), 2.72 (m, 2H), 2.33 (m, 2H), 2.11 (m, 2H), 1.89 (m, 2H), 1.69 (m, 2H), 1.45 (m, 10H), 1.3−1.1 (m, 56H), 0.94 (m, 8H), 0.78 (s, 6H), 0.47 ppm (s, 6H); ^{13}C NMR ($CDCl_3$, 75 MHz) 177.6, 177.0, 166.1, 164.6, 151.9, 144.5, 142.6, 131.6, 128.9, 127.9, 126.6, 125.4, 124.3, 122.0, 121.6, 118.9, 115.9, 104.1, 90.8, 90.4, 54.8, 54.3, 31.1, 29.0, 28.9, 28.2, 18.1, 17.1, 17.0, 16.7, 16.4, 13.5, 13.1, 12.7, 9.7, 9.5 ppm; UV−vis (CH_3CN, $c = 2.6 \times 10^{-5}$ M) λ_{max} (log ϵ) 266 (6.16), 326 (5.96), 407 (5.06), 430 (5.09); CD (CH_3CN, $c = 2.6 \times 10^{-5}$ M), nm ($\Delta\epsilon$) 228 (70), 260 (−129), 301 (23), 316 (−21), 348 (84), 432 (−6); HRMS (FAB) m/z calcd for $C_{84}H_{104}O_{18}Si_2$ 1456.6761, found 1456.6748.

Preparation of 11 from 7. Tetrabutylammonium fluoride in THF (0.89 mL, 1 M, 0.89 mmol) was added at 25 °C to a solution of **7** (520 mg, 0.357 mmol) in 20 mL of THF, and after the mixture had stirred for 1 min, the dark brown solution was quenched with 0.26 mL (2.14 mmol) of trimethylacetyl chloride. The solution, which immediately turned yellow, was stirred at 25 °C for 1 h. Diluted with 20 mL of ethyl acetate, it was washed with saturated aqueous $NaHCO_3$ and H_2O and dried (Na_2SO_4). Removal of the solvent left a dark yellow oil, which was purified by chromatography (eluent 1:2 ethyl acetate/hexanes). Obtained was 337 mg (72%) of (*M*)-(−)-**11**, a yellow solid, mp > 250 °C. Crystals were grown by dissolving (*M*)-(−)-**11** in a small amount of hot methanol. Hexanes were slowly added until the solution became cloudy. The solution was warmed until it became clear and allowed to cool slowly and evaporate at room temperature. Yellow crystals formed.

(*M*)-11: $[\alpha]_D$ −716 (c 0.0152, CH_3CN); IR (CCl_4) 2973, 1798, 1754, 1122, 1044 cm^{-1}; ^{1}H NMR ($CDCl_3$, 400 MHz) δ 8.22 (d, J = 8.5 Hz, 2H), 8.07 (d, J = 8.5 Hz, 2H), 8.02 (s, 2H), 6.99 (d, J = 8.3 Hz, 2H), 6.47 (d, J = 8.3 Hz, 2H), 2.78 (m, 2H), 2.39 (m, 2H), 2.09 (m, 2H), 1.85 (m, 2H), 1.55 (m, 2H), 1.53 (s, 18H), 1.38 (m, 4H), 1.36 (s, 6H), 1.25 (s, 6H), 1.23 (s, 6H), 0.93 (s, 6H), 0.82 (m, 2H), 0.63 ppm (s, 6H), 0.51 (s, 6H); ^{13}C NMR ($CDCl_3$, 75 MHz) 177.9, 177.0, 175.8, 166.2, 164.9, 146.5, 143.9, 143.7, 130.8, 127.4, 126.9, 126.3, 125.3, 123.9, 122.3, 120.5, 119.0, 117.6, 111.6, 91.4, 89.1, 55.0, 54.6, 54.4, 54.2, 39.8, 31.0, 29.7, 29.1, 28.6, 27.3, 16.9, 16.8, 16.2, 16.0, 9.8, 9.5 ppm; UV−vis (CH_3CN, $c = 2.1 \times 10^{-5}$ M) λ_{max} (log ϵ) 227 (6.16), 268 (6.23), 326 (6.03), 425 (3.78); CD (CH_3CN, $c = 2.1 \times 10^{-5}$ M), nm ($\Delta\epsilon$) 225 (−34), 251 (123), 297 (−19), 310 (2), 341 (−114), 428 (3); HRMS (FAB) m/z calcd for $C_{76}H_{80}O_{20}$ 1312.5243, found 1312.5237.

Preparation of 12 from 8. Similarly, 608 mg (0.418 mmol) of **8** gave 411 mg of (*P*)-**12** (75%), a yellow solid, mp > 250 °C. On TLC this isomer moves more slowly than **11**.

(*P*)-12: $[\alpha]_D$ 556 (c 0.0238, CH_3CN); IR (CCl_4) 2974, 1797, 1753, 1260, 1120, 1043 cm^{-1}; ^{1}H NMR ($CDCl_3$, 400 MHz) δ 8.29 (d, J = 8.5 Hz, 2H), 8.07 (d, J = 8.5 Hz, 2H), 7.81 (s, 2H), 6.97 (d, J = 8.3 Hz, 2H), 6.47 (d, J = 8.3 Hz, 2H), 2.76 (m, 2H), 2.42 (m, 2H), 2.12 (m, 2H), 1.89 (m, 2H), 1.65 (m, 4H), 1.53 (s, 18H), 1.44 (m, 2H), 1.35 (m, 2H), 1.27 (s, 6H), 1.26 (s, 6H), 1.24 (s, 6H), 0.90 (s, 6H), 0.70 (s, 6H), 0.20 ppm (s, 6H); ^{13}C NMR ($CDCl_3$, 75 MHz) 177.7, 177.2, 175.9, 166.6, 165.2, 146.7, 144.1, 143.7, 131.3, 127.9, 127.4, 125.9, 125.0, 124.5, 123.0, 121.2, 118.8, 117.9, 110.2, 91.1, 89.7, 55.0, 54.7, 54.0, 53.7, 40.0, 31.3, 29.7, 29.2, 28.5, 27.3, 17.1, 17.0, 16.4, 15.9, 9.8, 9.5 ppm; UV−vis (CH_3CN, $c = 3.1 \times 10^{-5}$ M) λ_{max} (log ϵ) 227 (6.04), 258 (6.08), 269 (6.09), 324 (6.91), 401 (3.61), 425 (4.44); CD (CH_3CN, $c = 3.1 \times 10^{-5}$ M), nm ($\Delta\epsilon$) 229 (77), 250 (−140), 299 (5), 311 (−14), 344 (101), 428 (−2); HRMS (FAB) m/z calcd for $C_{76}H_{80}O_{20}$ 1312.5243, found 1312.5221.

Crystal of 10. This was grown by allowing the solvent to evaporate at 25 °C over a period of a few days from an ethyl acetate solution of **10**.[10]

Crystal of 13. Warm hexanes were added to a concentrated solution of **13** in hot ethyl acetate until the solution turned cloudy. The solution became clear upon warming, and when allowed to cool slowly and evaporate through a loose cover, it precipitated crystals suitable for X-ray diffraction analysis.

Acknowledgment. We thank the National Science Foundation for a grant (CHE 98-02316), Dr. Alfred P. Bader for a Bader fellowship to K.P., and W. C. Still for advice.

Supporting Information Available: ^{13}C NMR, IR, UV, and CD spectra of **7**, **8**, **11**, and **12**. ^{1}H NMR spectra of **11** , **12**, and *p*-methoxyphenyl camphanate. HMQC spectra of **7**−**10**. Drawings of the conformations of **7**−**10** calculated to have the minimum energy. The chemical shifts of protons across from the camphanate groups in (*P*)- and (*M*)-helicenol camphanates. Lists identifying which of the two diastereomers has the lower R_f on silica gel for 19 pairs of helicenol camphanates. For **10**, **11**, and **13**, ORTEP diagrams, crystal data and structure refinement parameters, atomic coordinates, bond lengths and bond angles, anisotropic displacement coefficients, and H-atom coordinates. This material is available free of charge via the Internet at http://pubs.acs.org.

JO9919411